PROGRESS IN THE DEVELOPMENT OF HIGH DENSITY FUELS FOR ENHANCED ACCIDENT TOLERANCE

D.T.GODDARD, J.I.PAUL, R.LOGSDON,
National Nuclear Laboratory, Preston Laboratory,
Springfields, Preston, Lancashire, PR4 0XJ, UK

E.P.VERNON,
National Nuclear Laboratory, Chadwick House,
Birchwood Park, Warrington, Cheshire, WA3 6AE, UK

J.BUCKLEY, T.ABRAM,
School of Mechanical, Aerospace and Civil Engineering,
University of Manchester, Manchester M13 9PL, UK

S.RENNIE, E.LAWRENCE-BRIGHT, L.HARDING, R.SPRINGELL
University of Bristol Interface Analysis Centre, HH Wills Physics Laboratory,
Tyndall Avenue, Bristol, BS2 8BS, UK

Fuel materials with uranium densities higher than UO_2 could bring significant economic benefits to accident tolerant fuel concepts. The most promising candidate materials, UN and U_3Si_2, also have improved thermal properties compared to UO_2 resulting in additional safety benefits. This paper describes experimental studies of high temperature reactions between UF_6 and silicon which, if promising, might be used to develop a commercially scalable fabrication route for U_3Si_2 which avoids the need to use uranium metal. Investigations into optimising the pelleting procedures for U_3Si_2 are also outlined, using a conventional arc melted feedstock. In addition, a novel thin film approach has been used to fabricate idealised surfaces of uranium nitrides and oxides. The reaction of water (and hydrolysis products such as H_2O_2) with these surfaces has been studied using highly surface sensitive techniques, such as X-ray reflectivity and X-ray photoelectron spectroscopy revealing insights into the reaction mechanisms that are still debated within the literature.

1. Introduction

The aim of Accident Tolerant Fuels (ATF) research is to develop fuels which show improved performance under severe accident scenarios, whilst also benefitting fuel economics. Alternative fuel materials, such as uranium nitride (UN) and uranium silicide (U_3Si_2) are attractive due to their increased density (better economics) and superior thermal conductivity compared to standard UO_2 fuels [1,2]. However, the introduction of a new fuel type is non-trivial and requires significant investment in research and development to optimise fuel fabrication and to understand performance under irradiation in conditions relevant to the operation of light water reactors (LWRs). The most pressing challenges are:

1. Development of fabrication routes that are scalable for commercial deployment.
2. Understanding the mechanism of water reaction with the fuels, in case of pin failures and to underpin spent fuel storage.
3. Gather irradiation data on the fuels under LWR operating conditions and develop models to understand their behaviour.

Of the two favoured high density fuels UN has the higher uranium density (+40% relative to UO_2) however it is known to react rapidly with water at temperatures comparable with LWR operation and enrichment in ^{15}N would be required to avoid significant detrimental ^{14}C formation. Hence U_3Si_2 with a more modest (+17%) increase in uranium density is the current favoured option.

This paper outlines progress in the development of fabrication routes for U_3Si_2 and the use of thin film approaches to obtain a more detailed understanding of reaction mechanisms in the presence of oxidising species, initially focused on UN. The work has been undertaken through a Nuclear Innovation Programme in Advanced Fuels funded by the UK Government, Department of Business, Environment and Industrial Strategy, involving a collaboration between the National Nuclear Laboratory (NNL) and the Universities of Manchester and Bristol.

2. Manufacturing Routes for U_3Si_2

2.1. Routes from UF_6

An attractive route, if feasible, for the production of U_3Si_2 would be directly from uranium hexafluoride (UF_6), since this would eliminate the need for conversion of UF_6 to metallic uranium, as would be required if a conventional arc-melting process were to be followed. A thermodynamic assessment of the potential for UF_6 to react with elemental Si or gaseous silane (SiH_4) has been reported previously [3]. This indicated a number of reactions with a negative free energy of reaction that could potentially form uranium silicide compounds. Experimental studies of the reaction between uranium tetrafluoride (UF_4) and Si have also been undertaken [4] and showed the formation of silicide phases at temperatures of around 900°C. However, silicon rich uranium silicide phases, such as the trisilicide (USi_3) and disilicide (USi_{2-x}), formed preferentially with the likelihood of the desired U_3Si_2 phase being formed with further increases in temperature uncertain.

Experimental studies have been initiated at NNL to evaluate the reaction of UF_6 with Si using the purpose-built rig shown in Figure 1. The equipment is housed within an inert atmosphere glovebox providing protection for operators in case of leakage of UF_6, but also in case any of the reaction products are oxygen sensitive, as is known for uranium silicide compounds. Material selection for high temperature components in contact with UF_6 was given careful consideration. Nickel based alloys Inconel 600 and 601 were assessed using finite element modelling and used to inform the design of the reaction vessel. These materials have good high temperature strength and resistance to chemical attack from fluorides. Another element of the rig design was the sizing of the off-gas scrubber units used to capture unreacted UF_6 and reaction products, primarily silicon tetrafluoride (SiF_4). Sodium fluoride (NaF) pellets were used as the scrubber media due to its common use for trapping UF_6, however the effect of SiF_4 on the maximum loading factors are not well understood. Previous work [5] had indicated a loss of scrubber efficiency with combined UF_6/SiF_4 gas flows, but this was partly attributed to a difficulty in regenerating the pellets. A precautionary approach was adopted using a conservative value for the loading factor and a back-up scrubber unit.

The rig has been actively commissioned and the first operational tests carried out with the reaction vessel held at a temperature of 580°C, as recorded by a thermocouple placed within the bed of Si powder. Initial examination of the reaction product indicated the formation of a green coloured powder, readily identified by X-Ray Diffraction (XRD) as UF_4. This is consistent with thermodynamic predictions at this temperature as depicted in Figure 2.

2.2. Pelleting processes for U_3Si_2

Research at the University on Manchester has focused on synthesis via arc melting and fuel form fabrication through powder metallurgy, in a method similar to that reported by Harp et al. [6]. Material manufactured by this process will represent a base line for comparison with fuel forms manufactured by alternative techniques. The aim of this work is to develop

procedures for the fabrication of U_3Si_2 pellets with acceptable phase purity and density, in a reproducible manner, building on the findings of a similar study [7]. The use of a tungsten carbide milling vessel and media represent a deviation from what has previously been reported on in the literature.

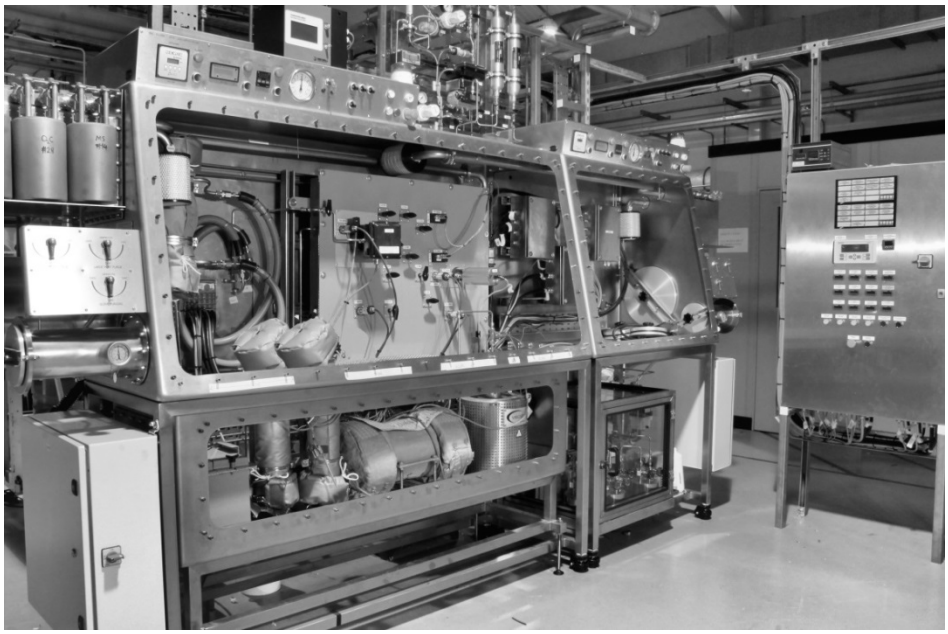

Figure 1: Photograph of the experimental rig to test reactions between UF_6 and Si.

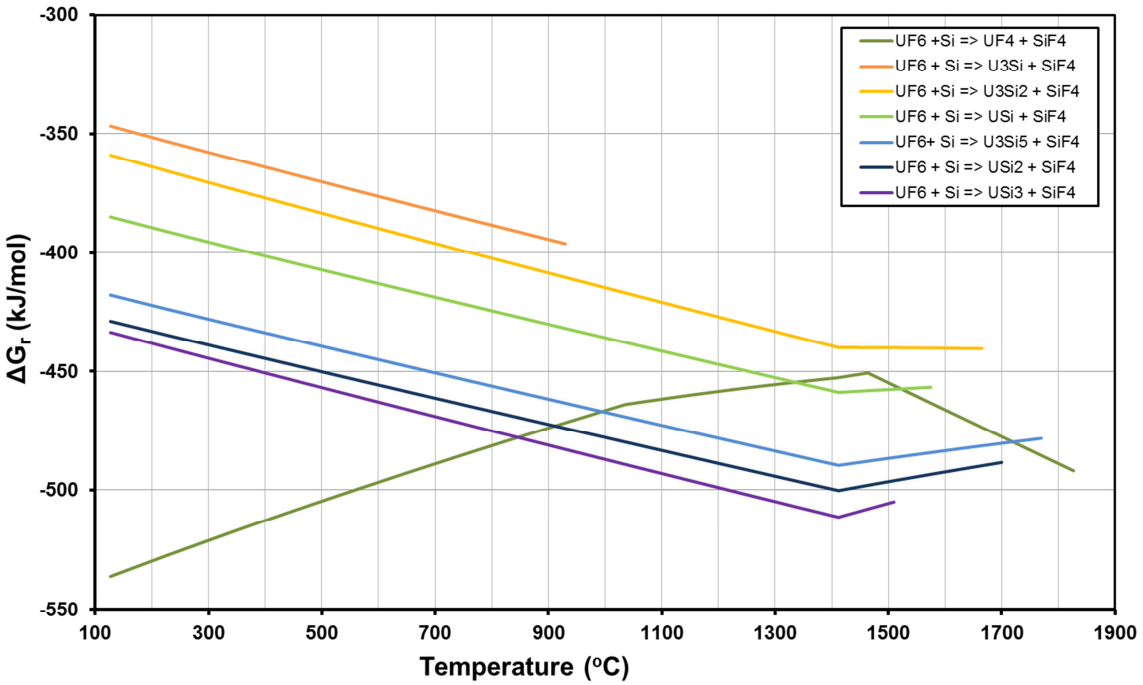

Figure 2: Calculated free energy of reaction (ΔG_r) as a function of temperature for various possible reactions between UF_6 and Si.

The uranium metal used in these preliminary studies was recycled from nickel-coated plates; with the nickel being removed via a mechanical process. The material was likely to contain contaminants, with Energy Dispersive X-Ray Analysis (EDX) indicating the presence of minor quantities of Ni, Al and Fe. U_3Si_2 was synthesised through arc melting in an argon atmosphere glovebox with O_2 and H_2O levels maintained below 10ppm throughout the process. Uranium pieces were melted on a water-cooled copper hearth with 7.5wt% Si, in the

form of lumps. A 300A arc was used to melt and simultaneously stir the material, the ingots were flipped and melted eight times to homogenise the melt. Figure 3A shows an ingot of uranium silicide following arc melting. A typical ingot size of 30-40g was produced per melt. The as melted material was crushed via pestle and mortar and then loaded into a 50ml tungsten carbide milling pot with ten tungsten carbide, 10mm diameter, milling media. The material was milled in a Retsch PM100 planetary ball mill for a total of 1 hour at 200 RPM with 1 minute intervals in each direction. Approximately 2.5g powder samples were pressed with a mechanical press at 360MPa to form 11.3mm diameter green pellets. The die bore and punch faces were lubricated with zinc stearate. The pellets were sintered in a R. D. Webb graphite insulated vacuum furnace. The pellets were loaded into a lidded graphite crucible on a bed of tantalum beads. The beads act as an oxygen getter during sintering and prevent interaction between the crucible and pellet, the setup is shown in Figure 3C. Pellets were sintered at 1500°C for 2 hours with a 20°C/min ramp rate in either a vacuum maintained below $3x10^{-3}$mbar or in a refreshed argon atmosphere. In addition to milling with the planetary mill a second stage of milling was performed with a Retsch MM400 mixer mill. A 2.5g charge was loaded in a 10ml stainless steel vessel with ten 5mm diameter milling media.

During the initial arc melting of individual uranium and silicon pieces some of the silicon component was ejected from the hearth, although this was small it may have resulted in depleting the silicon in the final ingot. Once coalesced into a single piece the arc melting process was found to be more consistent. The ingot itself was found to fracture during cooling, Figure 3A shows the ingot after melting. Figure 4 shows a micrograph of the U_3Si_2 powder following milling. A significant amount of material still remained as ~50µm fragments, some pieces as large as 150µm were also observed. Following completion of the milling run the majority of the original charge material was adhered to the walls of the milling vessel, Figure 3B. Of the 38.58g loaded into the vessel only 5.66g was free to pour from the vessel after the 1 hour milling run. The adhered material was removed through mechanical means. Investigation of the material milled in the MM400 showed a similar array of particle sizes but no larger (>100µm) particles were observed.

Table 1 provides data for density measurements taken for the green and sintered U_3Si_2 pellets. All pellets pressed to high densities and produced robust greens that were resistant to fracturing when handled, some chipping of the rim was evident on the final pellets. The pellet produced from the powder that underwent an additional stage of milling in the MM400 achieved a higher density compared to the other pellets. Density measurement via the Archimedes' method was not reliable due to the open porosity present in the sample. He-pycnometry measurements returned densities in the region of 95% of theoretical density for each of the pellets suggesting an open network of porosity existed.

Powder	**Sintering atmosphere**	**Green density**	**Sintered density**
PM100	Vacuum	71.2	81.0
PM100	Argon	68.8	80.8
PM100 + MM400	Argon	66.4	84.1

Table 1: U_3Si_2 Pellet Densities, measured geometrically and quoted as percent of theoretical U_3Si_2 density (12.2g/cm^3). All measurements have an associated uncertainty of ±0.5%.

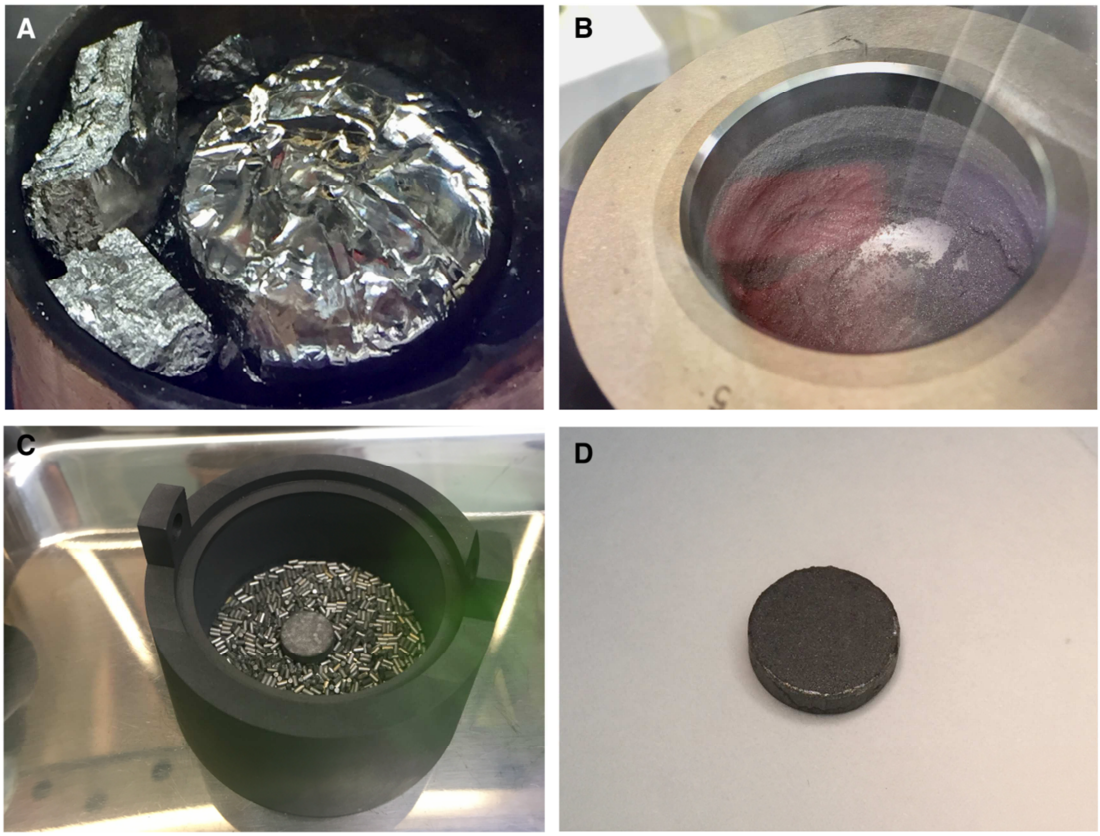

Figure 3: Various images taken from key steps of the U_3Si_2 manufacturing process. A) Arc-melted ingot fractured during cooling, B) Tungsten carbide milling vessel with powder adhered to walls, C) Crucible with tantalum beads and pellet, D) Vacuum sintered U_3Si_2 pellet with black coating.

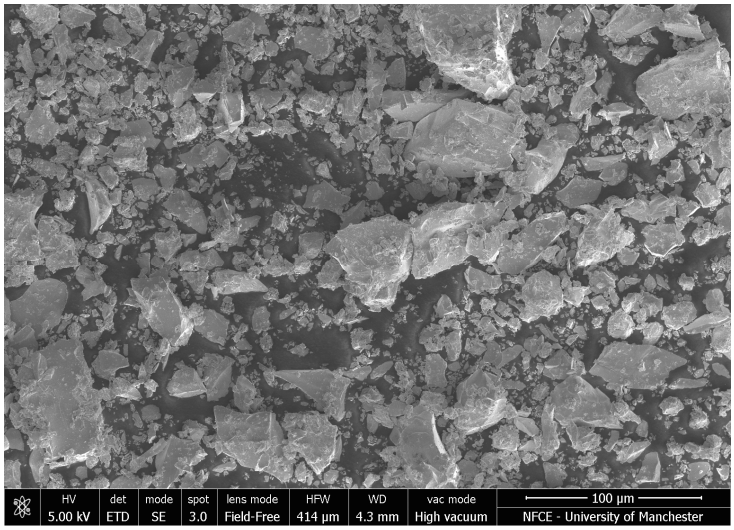

Figure 4: Secondary electron image of milled material following planetary ball milling with the tungsten carbide vessel and media.

XRD of arc melted material, crushed via pestle and mortar, showed the predominant phase present to be that of U_3Si_2, as can be seen in Figure 5. There was a noticeable shift in a number of peaks in the U_3Si_2 pattern compared to the reference. Refinement of the lattice parameters showed the shifts to be caused by an expansion of the c lattice parameter. This could possibly be caused by the existence of interstitials in this plane from impurities that were known to be present in the uranium source material. In addition to the U_3Si_2 peaks, two peaks at ~31.5° and ~36.5° were observed in the pattern suggesting the presence of an unidentified minor phase. The peak at 31.5° could be attributed the presence of USi_3[1], this aligns with the excess silicon incorporated in the original melt. The XRD pattern obtained for a pellet sintered in vacuum showed a decrease in the intensity associated with these minor phases but their presence still remained. The sintered material also contains peaks associated with UO_2, not present prior to heat treatment. Rietveld refinement of the pattern provided a calculated concentration of 1.2wt% UO_2, neglecting any component associated with the unidentified minor phase. The surface of the all pellets produced was coated in a layer of black material which was identified as uranium carbide via XRD analysis.

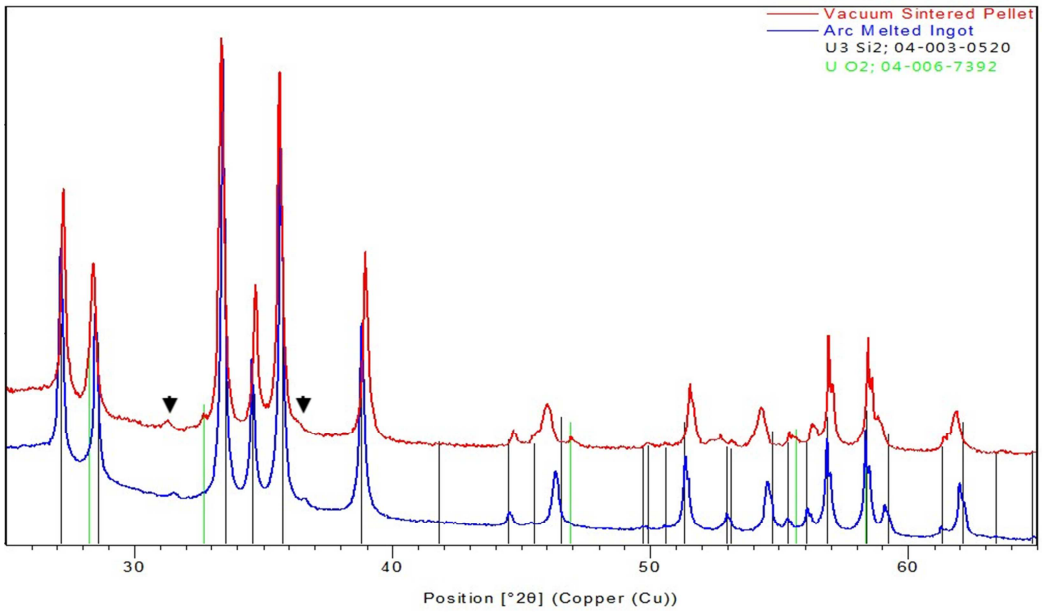

Figure 5: XRD patters obtained for the arc-melted material and vacuum sintered pellet. Both patterns show a strong match with the black lines from the tetragonal U_3Si_2 phase (PDF 04-003-0520) [8]. The vacuum sintered material contained peaks from a UO_2 phase indicated by the green lines (PDF 04-006-7392) [9]. The arrows indicate the presence of minor phases, more prominent in the arc-melted material.

The initial results from these early attempts to manufacture suitable U_3Si_2 pellets have demonstrated the capability to synthesise the desired phase via arc melting. The presence of an unidentified minor phase could be due to excess silicon or impurities in the material. The milling preformed in the tungsten carbide vessel appears to have been largely unsuccessful and is a possible contributory factor to the low sintered densities observed in the final pellets. The significant amount of powder adhesion to the walls of the mill vessel, >80% charge material, is possibly due to the combination of the hardness of the tungsten carbide and the high energy involved in the milling process at 200 RPM. Despite the poor morphology of the powder used it did press to high green density and produce robust pellets, although further work is required to optimise the sintered density.

[1] USi_3 X-ray diffraction pattern PDF 04-004-9084

3. A thin film approach to ATF research

Despite the progress that has been made in synthesising bulk UN and U_3Si_2, current methodologies often result in mixed-phase materials, rich in impurities. Given the complexity of these materials, it is difficult to assess the effect of individual impurities and study the behaviour of single phases in isolation. In this regard, thin films offer considerable potential, providing highly versatile, idealised samples that can be readily engineered to explore a wide range of material properties. Through varying the deposition parameters, it is possible to control the film microstructure, stoichiometry and impurity concentrations. Conducting nuclear material research on thin film systems therefore presents the opportunity to begin with a model surface, and incrementally introduce complexity such that individual parameters can be investigated in isolation. Such an approach enables the gap between theory and realistic scenarios to be bridged, with the aim of obtaining a more fundamental understanding of ATF behaviours.

In addition to allowing for single parameter investigations, the utilisation of thin films addresses many of the difficulties in handling radioactive samples. Given the ability to deposit thin films of thicknesses ranging from 0.1nm – 500nm, the sample activity is low in comparison with bulk materials, making them significantly easier to handle in a laboratory and transport to other facilities. At the University of Bristol thin films of UN and UO_2 have been prepared and initial investigations performed to compare their radiolytic dissolution behaviour.

3.1. Growth and characterisation

Thin films were grown using a DC magnetron sputter deposition system, comprising 4 individual sputter targets, allowing for both co-sputtering of materials and reactive sputtering of targets within gaseous environments. The results presented here highlight the progress made in the deposition of UN thin films, through reactive sputtering of a depleted uranium metal target in the presence of nitrogen gas.

Building on the recipe given by Black et al. [10], a series of growth optimisations were conducted to determine the optimal nitrogen pressure to deposit polycrystalline films of UN. Films were grown at room temperature by sputtering a uranium metal target in a reactive nitrogen atmosphere, on to 10mm x 10mm Corning glass substrates, purchased commercially from MTI Corp. XRD studies were performed to analyse the phases deposited using nitrogen pressures ranging from $2.0\text{x}10^{-5}$mbar to $1.0\text{x}10^{-3}$mbar, determining the optimal partial pressure for the deposition of single phase UN to be $2.0\text{x}10^{-5}$mbar.

In addition to the fabrication of single phase, polycrystalline samples, substrates with epitaxial matches to UN were selected to deposit single crystal films. To prevent oxidation of the nitride film, substrates that did not contain oxygen were specifically selected. Given bulk UN has a cubic crystallographic structure with a lattice parameter of 4.8897 Å, a $\sqrt{2}$ epitaxial match was obtained with the (001) Nb plane, which is also cubic with a lattice parameter of 3.300Å [11,12]. As shown on the right in Figure 6 this relation is achieved with a 45^0 rotation between the (001) UN and (001) Nb plane. As [001] Nb is known to grow epitaxially on [1-102] Al_2O_3 (Figure 6 (left)), the UN [001] film was grown on a [1-102] Al_2O_3 substrate with a [001] Nb intermediate buffer layer, acting as a barrier for oxygen diffusion in addition to providing an epitaxial buffer [13]. To deposit the Nb, the [1-102] Al_2O_3 substrate was heated to 800^0C, before being subsequently cooled to 500^0C in order to deposit the UN film. To prevent oxidation of the film, the sample was further capped with an additional 5nm layer of polycrystalline Nb, deposited at room temperature.

To characterise the sample, XRD and X-ray photoelectron spectroscopy studies (XPS) were conducted, with a full discussion of the results presented in [14]. XPS analysis showed the UN film to be stoichiometric, with only a small amount of oxide contamination present. The structure of the film was characterised with XRD, demonstrating the film to be both single

crystal and of single domain, with the epitaxial match of the substrate, buffer layer and film systems to be confirmed as that shown pictorially in Figure 6. However broad rocking curves were observed for both the [001] UN film and [001] Nb buffer layer, demonstrating a lack of coherence between the Nb buffer and Al_2O_3 substrate. As the quality of the UN film is limited by the quality of the Nb buffer, the epitaxial match between the substrate and the buffer layer must be addressed in order to improve the quality of the UN single crystal. However, as the growth of [001] Nb on [1-102] Al_2O_3 is shown to be optimised at 800^0C, it is unlikely that the quality of the UN film can be improved using this system, and alternative substrates must therefore be investigated. In addition to improving the quality of the single crystal UN films, further work will also focus on the deposition of uranium silicide phases, through co-deposition of uranium and silicon using DC magnetron sputtering.

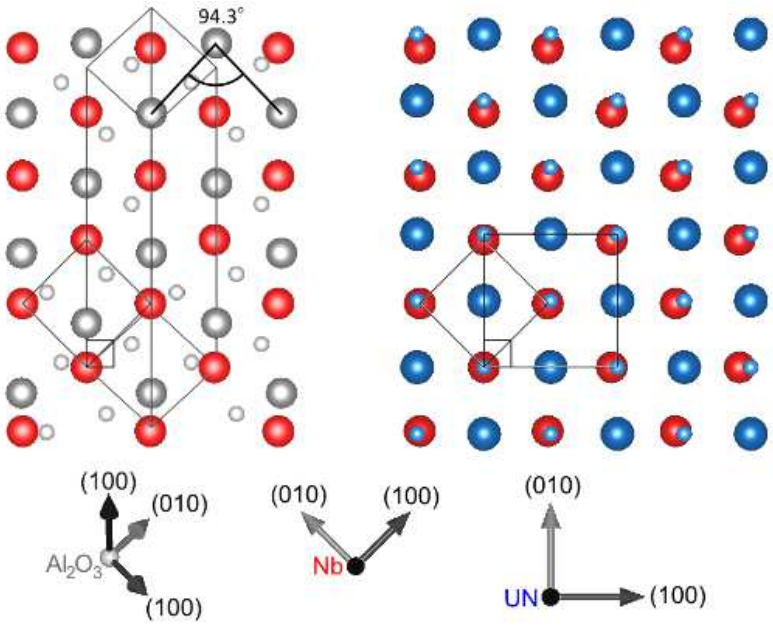

Figure 6: Model of (001) Nb on (1-102) Al_2O_3 (left) and (001) UN on (001) Nb (right, with Al_2O_3 shown in grey, Nb in red and UN in blue.

3.2. Thin film dissolution

One of the most significant concerns of using UN as an ATF is its high reactivity in water [15-17]. However no studies have been performed to assess the corrosion behaviour of UN under radiolytic conditions. Given that the fuel is most likely to be exposed to water in the presence of strong radiation fields, the effect of radiolytic species, including: H_2O_2, $OH^{\bullet}$, $O_2^{\bullet-}$, $HO_2^{\bullet}$, and O_2 must be considered. Such investigations are regularly performed for UO_2, which despite being insoluble in water, has been shown to corrode readily in the presence of radiolytic species [18-21]. To accurately assess the corrosion behaviour of UN, comparative radiolytic corrosion studies are therefore required.

To compare the radiolytic corrosion of UN with UO_2, polycrystalline UN and UO_2 thin films were exposed to H_2O_2, for a series of exposure times. X-ray reflectivity (XRR) profiles were recorded before and after exposure, to measure the change in film thickness, roughness and scattering length density (SLD) as a function of corrosion. Figure 7 shows the XRR scans, taken after exposing 600Å UN and UO_2 thin films to 0.1M H_2O_2 for 0, 250, and 6000s. For the UO_2 film, a dramatic increase in fringe separation is observed after 6000s, indicating significant decrease in film thickness. Comparing this with the UN profile, fringe separation is also observed to increase, however at a much slower rate indicating less material has been corroded. Through modelling the data using the GenX reflectivity software [22] SLD plots were calculated, displaying the films behaviour more clearly. As shown in the inset of Figure 7, the SLD plots show the UO_2 film to have almost been completely removed after 6000s,

whereas only ~150Å of the UN film is removed over the same exposure period. This result is in contrast with literature showing UN to corrode faster than UO_2 in water and indicates that UN could be more corrosion resistant in an accident scenario than previously considered.

In addition to displaying the change in film thickness, the SLD plots also demonstrate the change in roughness at the surface of the films, with the UO_2 film shown to undergo more significant surface roughening in contrast with UN. This is further discussed in [23], where along with the full results of the work presented here, a U_2N_3 film has additionally been investigated to provide insight into the corrosion mechanism of UN.

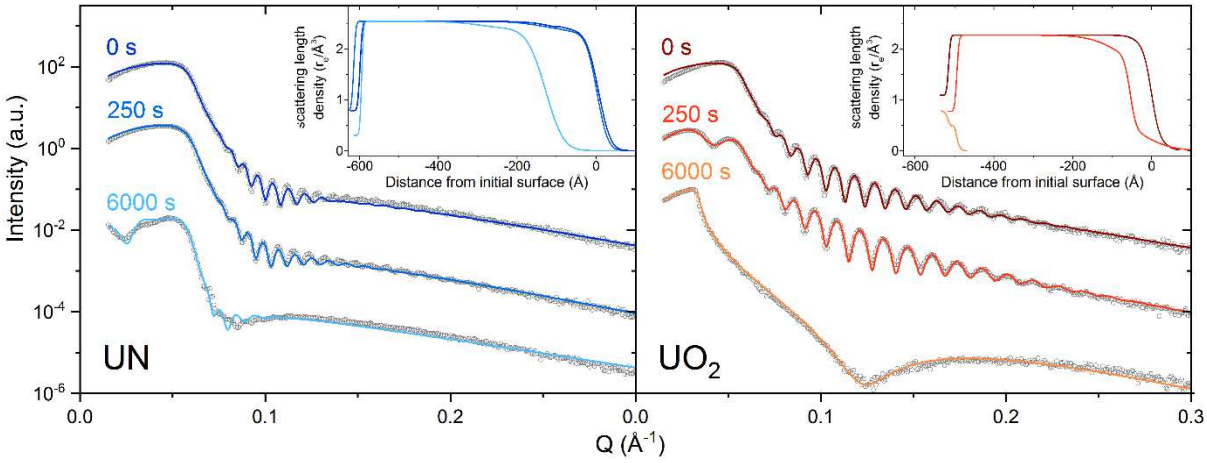

Figure 7: XRR data taken after 0s, 250s, and 6000s exposure of 0.1M H_2O_2 solution to UN and UO_2 thin films. The data are represented as open grey circles and the fits as blue and red solid lines for the UN and UO_2 samples, respectively.

4. Conclusions

The use of high density fuels as part of ATF concepts has significant potential to improve both the safety and economic performance of nuclear plants. The work presented here highlights some of the challenges that will need to be overcome in the manufacture of U_3Si_2 fuels. Progress has been made in the construction of a test facility for studying conversion processes directly from UF_6, although high temperatures are expected to be required, with associated materials challenges.

The pelleting of near phase pure U_3Si_2 from arc melted ingots has been demonstrated. Milling of powders using tungsten carbide mill vessels and media led to considerable adhesion of the powder to the walls. Despite this the powder formed strong green pellets which could be sintered to a reasonable density, albeit with some open porosity. Further development and optimisation of pelleting processes will be necessary to meet target specifications for the fuel.

ATF thin films of UN, both polycrystalline and single crystal, having been deposited. It has been demonstrated through initial studies simulating radiolytic corrosion, that these idealised samples present an opportunity to explore the properties of high density fuels without the complexities of working with bulk materials. As such, thin films could be highly advantageous for the nuclear research community, allowing wider access to ATF materials, and providing idealised surfaces on which to conduct single parameter studies.

5. References

[1] S.L.Hayes, J.K.Thomas and K.L.Peddicord, Material property correlations for uranium mononitride, *J. Nucl. Mater,* vol. 171, pp. 289-299, 1990.
[2] J.T.White, A.T.Nelson, J.T.Dunwoody, D.D.Byler, D.J.Safarik, K.J.McClelland, Thermophysical properties of U_3Si_2 to 1773K, *J. Nucl. Mater,* vol. 464, pp. 275-280, 2015.

[3] H.R.Foxhall, S.L.Owens and D.T.Goddard, Thermodynamic modelling of a single-stage production route for U_3Si_2 accident tolerant fuel, Proceedings of Topfuel 2015, Zurich, Switzerland, 2015.
[4] D.T.Goddard, D.P.Mathers, D.G.Eaves, P.Xu, E.J.Lahoda and J.M.Harp, Manufacturability of U_3Si_2 and its high temperature oxidation behaviour, Proceedings of Topfuel 2016, Boise, Idaho, USA, 2016.
[5] R.M.Schultz, W.E.Hobbs, J.L.Norton and M.J.Stephenson, Sorbent selection and design considerations for uranium trapping, Union Carbide-Nuclear Division, Report K/ET-5025, 1981.
[6] J.M.Harp, P.A.Lessing, B.H.Park, and J.Maupin, Preliminary investigation of candidate materials for use in accident resistant fuel, *LWR Fuel Perform. Meet. 2013*, pp. 757–762, 2013.
[7] J.M.Harp, P.A.Lessing, and R.E.Hoggan, Uranium silicide pellet fabrication by powder metallurgy for accident tolerant fuel evaluation and irradiation, *J. Nucl. Mater,* vol. 466, pp. 728-738, 2015.
[8] W.H.Zachariasen, Crystal chemical studies of the 5f -series of elements. VIII. Crystal structure studies of uranium silicides and of $CeSi_2$, $NpSi_2$, and $PuSi_2$, *Acta Crystallogr.*, vol 2, no 2, pp 94–99, 1949.
[9] J.S.Anderson, I.F.Ferguson and L.E.J.Roberts, Anionic vacancies in fluorite-type oxides, *J. Inorg. Nucl. Chem.*, vol 1, no 4, pp 340–341, 1955.
[10] L.Black, F.Miserque, T.Gouder, L.Havela, J.Rebizant, and F.Wastin, Preparation and photoelectron spectroscopy study of UN_x thin films, *J. Alloys Compd*, vol. 315(1-2), pp. 36-41, 2001.
[11] J.Williams and R.A.J.Sambell, The uranium monocarbide-uranium mononitride system,. *J. Less-Common Metals*, vol. 1, pp. 217-226, 1959.
[12] R.L.Barns, Niobium: Lattice Parameter and Density, *J. Appl. Phys.*, vol. 39, pp. 4044,, 1968.
[13] A.R.Wildes, J.Mayer, and K.Theis-Bröhl. The growth and structure of epitaxial niobium on sapphire, *Thin Solid Films*, vol. 401 no. 1-2, pp. 7-34, 2001.
[14] E.Lawrence Bright, S.Rennie, M.Cattelan, N.A.Fox, D.T.Goddard, R.Springell, Epitaxial UN and α-U_2N_3, *Thin Solid Films,* vol. 661, pp. 71-77, 2018.
[15] S.Sugihara and S.Imoto, Hydrolysis of uranium nitrides, *J. Nucl. Sci. Technol.* vol. 6, no. 5, pp. 237-242, 1969.
[16] S.Sunder and N.Miller, XPS and XRD studies of corrosion of uranium nitride by water, *J. Alloys Compd.* vol. 271-273, pp. 568-572, 1998.
[17] M.Jolkkonen, P.Malkki, K.Johnson, J.Wallenius, Uranium nitride fuels in superheated steam, *J. Nucl. Sci. Technol.* vol. 54, no. 5, pp. 513-519, 2017.
[18] D.W.Shoesmith and S.Sunder, The prediction of nuclear fuel (UO_2) dissolution rates under waste disposal conditions, *J. Nucl. Mater.* vol. 190, pp. 20-35, 1992.
[19] S.Sunder, D.Shoesmith and N.Miller, Oxidation and dissolution of nuclear fuel (UO_2) by the products of the alpha radiolysis of water, *J. Nucl. Mater.* vol. 244, no. 1, pp. 66-74, 1997.
[20] D.W.Shoesmith, Fuel corrosion processes under waste disposal conditions, *J. Nucl. Mater.* vol. 282, no. 1, pp. 1-31, 2000.
[21] R.Springell, S.Rennie, L.Costelle, J.Darnbrough, C.Stitt, E.Cocklin, C.Lucas, R.Burrows, H.Sims, D.Wermeille, J.Rawle, C.Nicklin, W.Nuttall, T. Scott and G.Lander, Water corrosion of spent nuclear fuel: radiolysis driven dissolution at the UO_2 /water interface, *Faraday Discuss.* vol. 180, pp. 301-311, 2015.
[22] M.Björck and G.Andersson, GenX: An extensible X-ray reflectivity refinement program utilizing differential evolution, *J. Appl. Crystallogr.* vol. 40, no. 6, pp. 1174-1178, 2007.
[23] E.Lawrence Bright, S.Rennie, A.Siberry, K.Samani, K.Clarke, D.T.Goddard and R.Springell, Corrosion of Nuclear Fuels: The Interaction of Uranium Nitride and Uranium Dioxide Surfaces with H_2O_2, 2018, [in preparation].